Research Article

Innovative Chitosan–Caffeic Acid Phenyl Ester Nanocomposite as a Sustainable Tool against Charcoal Rot Disease of Sunflower in Egypt

Sally M. Amer[1], Heba Yousef[1]*, Germine M. Hamdy[2], Rehab R. Abdrabou[2] and Said S. Moselhy[2]

[1]Central Laboratory for Biotechnology, Plant Pathology Research Institute, Agriculture Research Center, Giza, Egypt; [2]Biochemistry Department, Faculty of Science, Ain Shams University, 1 EL Gamma st., Giza, 12619, Abbaseya, Cairo 11517, Egypt.

Abstract | The growing problems of environmental pollution and resistance to fungicides in sunflower farming draw attention to the necessity of the sustainable level of disease control. The aim of this study was to examine the production, characterization, and biological performance of chitosan-based nanocomposites incorporated with caffeic acid phenethyl ester (CH -CAPE NPs) to control the growth of *Macrophomina phaseolina*; a fungus that causes charcoal rot in the sunflower (*Helianthus annuus* L.). The features of chitosan nanoparticles (CH NPs), CAPE nanoparticles (CAPE NPs), and CH-CAPE nanocomposites were measured using Fourier Transform Infrared (FTIR), UV- Visible spectroscopy, scanning electron microscopy (SEM), and zeta potential (ZP). The uniform and well dispersed spherical structures of the NPs had an average size of 58.4 nm. *In vitro* antifungal assay indicated that CAPE NPs at 100 µg/ml completely inhibited (100%) *M. phaseolina* mycelial growth, which was better than CH NPs (80%) and CH-CAPE NPs (85%). Field experiments conducted in Giza governorate, Egypt, in 2023 and 2024 growing seasons revealed that CAPE NPs remarkably increased the growth parameters of sunflower, including height of plant, head diameter, and total yield of the plant relative to the controls. Biochemical measurements indicated that there was an increased phenols and sugar accumulation, and high peroxidase, polyphenol oxidase, and catalase activities, displaying an improvement in systemic acquired resistance (SAR). Microscopic analysis also established enhanced vascular integrity and root growth, while fungal colonization was absent in the treated plants. The results acquired indicated that CAPE NPs had strong antifungal and defense-stimulating effects, considered as a long-term and ecofriendly nanobiotechnological strategy used to manage the soil-borne pathogen in the sunflower production field in the most effective way.

Received | March 03, 2026; **Revised** | March 25, 2026; **Accepted** | April 02, 2026; **Published** | April 14, 2026
***Correspondence** | Heba Yousef, Central Laboratory for Biotechnology, Plant Pathology Research Institute, Agriculture Research Center, Giza, Egypt; **Email:** heba.yousef@live.com
Citation | Amer, S.A., H. Yousef, G.M. Hamdy, R.R. Abdrabou and S.S. Moselhy. 2026. Innovative chitosan–caffeic acid phenyl ester nanocomposite as a sustainable tool against charcoal rot disease of sunflower in Egypt. *Novel Research in Microbiology Journal*, 10(2): 232-252.
DOI | https://dx.doi.org/10.17582/journal.nrmj/2026/10.2.232.252
Keywords | Sunflower, *Macrophomina phaseolina*, Charcoal rot, Chitosan nanoparticles, Caffeic acid phenethyl ester, Nanocomposites

Copyright: 2026 by the authors. Licensee ResearchersLinks Ltd, England, UK.
This article is an open access article distributed under the terms and conditions of the Creative Commons Attribution (CC BY) license (https://creativecommons.org/licenses/by/4.0/).

Introduction

Sunflower (*Helianthus annuus* L.) is a remarkable oilseed crop that is grown on over 28 million hectares and ranks fourth in the world for oilseed output (Yousef, 2021). Because of its well-developed root system and ability to adapt to a variety of agroecological conditions, it is more suitable for

temperate and semi-arid climates (Cvejić *et al.*, 2024). Due to the country's limited domestic oil output and fast population expansion, Egypt is trying to meet the growing demand for vegetable oils, making sunflower farming more important (Nurah *et al.*, 2022). Despite this potential, environmental restrictions, disease pressures, and economic limits provide serious obstacles to the Egypt's sunflower production, causing a detrimental effect on crop productivity and oil quality (Bán *et al.*, 2023).

One of the most damaging biotic stresses affecting sunflowers is charcoal rot, is brought on by the soil-borne necrotrophic fungus *Macrophomina phaseolina* (Tassi) Goid (Ali *et al.*, 2022). Egyptian agroecosystems frequently experience high temperatures and drought, making the fungus very aggressive. Under these conditions, the fungus causes root and stem rot, resulting in total crop loss and notable decreases in seed weight, quantity, and oil content. Disease control is very difficult since *M. phaseolina* can spread by contaminated seeds or direct contact with the soil, and it can survive for extended periods of time in soil due to its resilient microsclerotia (Mahdy *et al.*, 2023).

The pathogen's significance as a worldwide threat to agricultural sustainability is further increased by its remarkably large host range, infecting about 500 to 700 plant species, in addition to its wide geographic spread (Samy *et al.*, 2025). When infection starts, *M. phaseolina* particularly in warm, dry environments can quickly invade the sunflower tissues, frequently within 24 to 48 h. Premature ripening, decreased head diameter, loss of green coloration in stems, grey discoloration moving upward from the stem base, and degradation or absence of pith tissue are some of the symptoms that are usually manifested in sunflower fields after the seed-filling stage (Cvejić *et al.*, 2024). Presence of the pathogen is confirmed by the observation of microsclerotia on the main roots and within the stem tissues.

Charcoal rot-related yield losses vary greatly depending on the severity of infection and environmental factors. Severe outbreaks can result in catastrophic losses of 75–90% in crop yield. Meanwhile, moderate infections frequently cause yield decreases of up to 20% (Samy *et al.*, 2025). The management options are limited, and once the plant reaches the reproductive and maturation stages, intervention becomes challenging, because the symptoms are frequently manifested late in the growing season (Cvejić *et al.*, 2024). *M. phaseolina* infection is the result of the pathogen's ability to stay in soil, flourishes under conditions of heat and drought, and infects a variety of hosts, representing a considerable barrier to Egypt's sunflower production and a persistent danger to the stability of the world's oilseed crops. Currently, disease management strategies heavily rely on chemical fungicides, posing environmental hazards, health risks, and high potential of resistance development among the pathogens. Furthermore, excessive use of chemical fertilizers to enhance crop yield has led to soil degradation, microbial imbalance, and environmental pollution in the Egyptian farmlands (El-Rayes *et al.*, 2022). Therefore, there is an urgent need for ecofriendly, sustainable alternatives that maintain or improve crop health while minimizing the ecological footprints.

Chitosan; a biodegradable polysaccharide derived from chitin, has emerged as a promising natural biopolymer with inherent antimicrobial and plant growth-promoting properties (El-Hadrami *et al.*, 2010). Chitosan-based nanocomposites can act both as antifungal agents and carriers for bioactive compounds, improving their stability, bioavailability, and targeted delivery (Farhatun *et al.*, 2020). The integration of chitosan nanomaterials with phenolic compounds such as caffeic acid; a naturally occurring antioxidant and antifungal agent found in numerous plants, holds the potential for synergistic effects in enhancing plant defense mechanisms against microbial pathogens (Riaz *et al.*, 2019). Caffeic acid modulates lignification, reinforces cell walls, and scavenges reactive oxygen species (ROS), thereby mitigating pathogen invasion and oxidative stress (Ibrahim *et al.*, 2021). The objective of the present study was to develop an integrated, ecosustainable disease management strategy for sunflower charcoal rot in Egypt, through using chitosan-based nanocomposites enriched with caffeic acid.

Materials and Methods

Isolation of the sunflower charcoal rot-inducing pathogen

Ten sunflower plants exhibiting typical symptoms of charcoal rot were collected from Giza fields for pathogen isolation. To isolate *Macrophomina phaseolina*, seven small (0.5 cm diam.) epidermal sections were excised from the infected tissues using a sterile scalpel, surface-sterilized in 75% ethanol for 30

sec, followed by 2.5% sodium hypochlorite for 30 sec, and then rinsed in sterile distilled water for 1 min. The disinfected sections were placed on potato dextrose agar (PDA) supplemented with chloramphenicol (0.1 mg/ml) to inhibit bacterial growth. Plates were incubated at 28 ˚C in darkness for 5 d. After incubation, the emerging fungal colonies were purified using the hyphal tip method and identified based on their morphological characteristics, as described by Dhingra and Sinclair (1973).

Molecular identification of the fungal pathogen

The genomic DNA of *M. phaseolina* isolate was extracted from single spore fungal cultures grown on PDA medium using a DNeasy Plant Mini Kit (Qiagen-Hilden-Germany). To confirm the identity of *M. phaseolina*, specific polymerase chain reaction (PCR) analysis was performed using two primers specific for *M. phaseolina*; F: (5′-CCGCCAGAGGACTATCAAAC-3′) and R: (5′-CGTCCGAAGCGAGGTGTATT-3′), as described by Yousef (2021). The primer amplified 350 bp fragments from all typical isolates of *M. phaseolina*. PCR amplifications were performed using 7 µl of GoTaq® Green Master Mix (2X) (Promega Corporation, Madison, USA), 14 µl of nuclease-free water, 1 µl of each of the forward and reverse primers, and 2 µl of DNA template. DNA amplification was carried out using a thermal cycler. Amplification was conducted through initial denaturation at 95 ˚C for 4 min followed by annealing step 45 cycles at 94 ˚C for 1 min, 55 ˚C for 1 min, 72 ˚C for 2 min, and a final extension step at 72 ˚C for 5 min. All PCR reaction products were electrophoresed on 1% agarose gel, stained with ethidium bromide, and visualized under UV light.

Preparation of the nanoparticles and nanocomposites

Synthesis of chitosan nanoparticles (CH NPs)

Chitosan NPs were prepared *via* ionotropic chitosan gelation with sodium tripolyphosphate (TPP) anions. Chitosan (0.2%) was mixed in ascorbic acid (1%) solution and agitated at room temperature for 1 h (1000 rpm). A TPP stock solution was made by dissolving 0.03 g of TPP in 11 mL of dist. water. CH NPs were formed spontaneously when 1 ml of TPP stock solution was added dropwise to chitosan solution while stirring at 1000 rpm for 1 h at room temperature. The CH NPs were then sonicated for 1 h to separate their tiny sized particles (Calvo *et al.*, 1997).

Synthesis of caffeic acid phenyl ester nanoparticles (CAPE-NPs)

To prepare CAPE-NPS, 10 mg of caffeic acid phenyl ester were dissolved in 10 ml of absolute ethanol, and sonicated for 1 h at room temperature (20–25˚C) using ultrasonic power at a frequency of 50 kHz (XUBA3Analogue Ulta-sonic Bath, Grant Company, Saint Joseph, MO, USA) (Shoala *et al.*, 2025).

Synthesis of chitosan- caffeic acid phenyl ester nanocomposite

While the CH-NPS solution was being stirred at 400 rpm, TPP and CAPE-NPS were added dropwise using a syringe. The mixed system was maintained at 600 rpm for 8 h at room temperature using an ultrasonic sonicator (Elmasonic S 30 H, Elma, Germany) to ensure their homogeneity and separation of their tiny sized particles. The pH was adjusted to 4-5 to enhance the stability of the formed nanocomposite. Afterward, the mixture was centrifuged at 16.100 x g for 20-30 min to collect the composite, the composite was washed with dist. water to remove excess materials, and finally the formed nanocomposite was dried using a freeze dryer (Nguyen *et al.*, 2022).

Characterization of the nanoparticles and nanocomposite

Transmission electron microscope (TEM)

Characterization of the prepared nanomaterials was performed *via* analyzing their structural, morphological, and surface properties. Their shape and texture were scanned through the high-resolution Transmission Electron Microscope (HRTEM, JEOL TEM-2100, Japan) with an accelerating voltage of 250 kV and magnification of 20 X. The nanomaterials were prepared before measurement by a sonication prop under conditions of pulse -every 1 seconds [pulse mode (1 s on / 1 s off)] at 85% amplitude power and at maximum temperature for 30 min. Finally, 50 µl of each nanocomposite were individually added to TEM grid with air drying for 5 h at room temperature (Youssef *et al.*, 2021).

X-ray diffraction (XRD) technique

Chemical structure of the prepared NPs was evaluated using the X-ray diffraction (XRD) technique. The integrated NPs were studied for deciding the design creation and the translucent stage utilizing a X-beam diffractometer (XRD, D8-Find, Bruker, with CuKα radiation (1.5418 Å), Madison, WI, USA) working at a current of 40 MA, voltage of 40 kV, and step filter

0.01º. In any case, the dried nanocomposite samples should be ready before estimation, where tests processing were conducted utilizing basic planetary ball factory (LZQM0.4L, Shicheng Desert Spring Mineral Gear Assembling Co., Ltd.), in which ball factory of treated steel (0.1 cm breadth) was placed in a processing measure with tests for 1 h at 1500 rpm, as described by Ismail *et al.* (2021).

Dynamic light scattering (DLS)

In dynamic light scattering (DLS) analysis, the sample suspension was illuminated by a laser beam, after which the laser light was scattered in all directions. The light scattering was observed at a certain angle over time. Signal variation was attributed to the random Brownian motion of the NPs. The angular intensity distribution was used to determine the particle size by the Stokes-Einstein equation. DLS was carried out using particle size analyzer (Malvern Panalytical Ltd. Model of NanoSight NS500, UK), in reference to El-Wakeel *et al.* (2022).

Zeta potential (ZP)

Zeta potential (ZP) was used to describe the dispersion stability of the nanocomposite. ZP was conducted using zeta sizer analyzer (Malvern Panalytical Ltd. Model of NanoSight NS500, UK), following the methodology previously described by Rahman *et al.* (2022).

FTIR-ATR and UV–visible spectroscopic analysis of CAPE–chitosan nanocomposite

The encapsulation efficiency of CAPE within the chitosan matrix was evaluated using Fourier Transform Infrared Spectroscopy with Attenuated Total Reflectance (FTIR-ATR) and UV–Visible spectroscopy (Raza *et al.*, 2020).

Effect of different concentrations of bulk, nanoparticles, and composite-based NPs on in vitro growth of M. phaseolina

A sterile cork borer (4 mm diam.) was used to cut a mycelial disc from the actively growing margins of a 7-days old *M. phaseolina* culture. A disc was aseptically placed at the center of each PDA plate previously seeded with the respective nanomaterial concentration. Working concentrations of namomaterials involved; 50, 100, and 200 µg/ml. These seeded plates were prepared using the amended-media technique, in which the required volume of each liquid nanomaterial was added aseptically to molten PDA cooled to 45–50 ˚C and gently swirled to ensure uniform distribution. The seeded medium was poured into petri plates and allowed to solidify, while control plates consisted of PDA only. The plates were incubated for 10 d at 25 ± 2˚C. After incubation, the radial mycelial growth of the pathogen in NPs supplemented plates was measured (cm) in each plate using a calibrated ruler and compared to the control plate (Karibasappa *et al.*, 2020). Three replication of each treatment were tested, and mean values were recorded (±SD). The percentage reduction (%) in colony diameter was calculated using the following formula reported by Oubou *et al.* (2018):

$$\text{Reduction \%} = [Gc–Gt/\ Gc] \times 100$$

Where; Gc = growth diameter in the control plate; Gt = growth diameter in the treated plate.

Field experiment

To study the effects of NPs and nanocomposite on controlling charcoal rot disease infecting sunflower seeds and the resultant effects on plant growth parameters, a field experiment was performed in the Agricultural Research Center, Giza governorate for two successive seasons (2023/2024). The used soil type was sandy clay [34.7% clay, 31.9% sand, 29.8% silt pH 8.44, and Electrical Conductivity (Ec) of 5.75]. The experiment was conducted in a randomized complete block design with three replicate per treatment. Each plot consisted of 3 rows, 50 cm wide, and 3.5 m long. Sunflower seeds (*cv.* 162) were dipped individually in each nanocomposite treatment for 50 min before sowing in presence of 2% (w/v) arabic gum solution as a sticking agent. Treated sunflower seeds were transplanted in plots at the rate of 5 seeds/ plot, with three replicate each. Pots involving untreated sunflower seeds were used as controls. All agricultural practices were performed based on the Egyptian Ministry of Agriculture's recommendations.

Experimental design

Plots were planted with 2-3 seeds/hill of sunflower. The nanomaterial treatment's solutions were prepared at a concentration of 100 µg/ml, which was selected as a moderate and commonly used level. The grown plants (2-weekss old) were sprayed with each treatment individually for 2 times, the first at the 40th day when the sunflower reached the phenological growth phase of leaf development, and the second on the 80th day when there was stems elongation with

flower-bud formation (Kolenčík *et al*., 2020; Yousef, 2021). Plots were sprayed with tap water as controls. Another set of plots was treated with Rizolex-T fungicide (50% WP) (Tolclofos-methyl 20% + thiram 30%) at a dose of 3g/kg as positive controls. After 60 d from planting, fresh and dry weights of shoots and roots were determined, and shoot and root length were recorded using a calibrated ruler. The treatment groups were divided into a control (untreated) group and seven other treated groups for each pot as follow: caffeic acid phenethyl ester (CAPE), caffeic acid phenethyl ester nanoparticles (CAPE-NPs), Chitosan (CH), chitosan nanoparticles (CH-NPs), caffeic acid phenethyl ester-chitosan composite (CH-CAPE), chitosan caffeic acid phenethyl ester nanocomposite (CH-CAPE-NPs), and a fungicide (Rizolex T50).

Disease assessments

Disease incidence was calculated for each treatment according to the following equation:

$$\text{Disease incidence (\%)} = a/A \times 100$$

Where; a = number of diseased plants, and A = total number of evaluated plants.

This formula was used to determine the percentage of infected plants after 60 d from planting according to Darwesh and El-Shahawy (2023).

Biochemical analyses

Preparation of enzyme extract

Enzyme extracts were prepared following the method reported by Maxwell and Bateman (1967). Each treatment's dry tissues (0.5 g) were ground in a mortar with 3 ml sodium phosphate buffer at pH 6.8, and centrifuged at 100 g for 20 min at 6°C. For enzyme assays, the resulting supernatant fluids were processed.

Peroxidase activity (POD)

The activity of peroxidase (POD) was measured calorimetrically at 430 nm based on the oxidation of pyrogallol to pyrogalline using H_2O_2 (Thimmaiah, 1999). The reaction mixture contained 0.5 ml of 0.1 M sodium phosphate buffer at pH=7.0, 0.3 ml enzyme extract, 0.3 ml of 0.05 M pyrogallol, and 0.1 ml of 1.0% H_2O_2, and completed with a buffer up to 3.0 ml. Optical density was measured in all the test tubes. The increase in the absorbance at 430 nm was recorded against a blank with phosphate buffer instead of an enzyme extract. One unit of enzyme activity was expressed as changes in absorbance/min at 425 nm at 25°C under standard assay conditions.

Polyphenol oxidase activity (PPO)

The activity of polyphenol oxidase (PPO) was calculated using the colorimetric method described by Maxwell and Bateman (1967). The reaction mixture contained 1.0 ml sample extract, 1.0 ml of 0.2 M sodium phosphate buffer at pH= 7.0, 1.0 ml of 10-3 M catechol, and completed to a final volume of 6.0 ml with buffer. The mixture was incubated for 30 min at 30°C. The amount of the enzyme that produced an increase of 0.001 absorbance units/ min at 25°C was recorded as one unit of enzyme activity.

Catalase (CAT) activity

The activity of catalase (CAT) enzyme was determined as described by Aebi (1974). 0.1 ml of the enzyme extract was added to 2.9 ml of a reaction mixture containing 0.3M H_2O_2 (5%) and 0.5M sodium phosphate buffer (pH 7.6). The activity of catalase was measured by monitoring the reduction in absorbance at 240 nm as a result of H_2O_2 consumption. CAT activity was expressed as Unit/min/mg/protein. One unit of enzyme activity was defined as the decomposition of 1µmol of H_2O_2 / min.

Determination of the phenolic contents

Free, conjugated, and total phenols were determined by mixing 1 ml of the sample extract with 0.25 ml HCl, boiled in a water bath for 10 minutes, and left to cool. 1 ml of the folin reagent and 6 ml Na_2CO_3, were added. The mixture was completed to a final volume of 10 ml using dist. water. Color optical density of the reacted mixture was measured at 520 nm using a spectrophotometer (Spectronic 601, Milton Roy, USA). Phenol contents were determined as mg/g fresh weight/min (Zieslin and Ben-Zaken, 1993).

Determination of the carbohydrates

Total carbohydrates assay protocol was conducted according to the method of Anthrone, described by McCready *et al*. (1950). Carbohydrates were first hydrolyzed into simple sugars using dilute hydrochloric acid. In hot acidic medium, glucose was dehydrated to hydroxymethyl furfural. This compound with anthrone formed a green colored product with an absorption maximum at 630 nm. The samples were ground into a powder and mixed with 80% ethanol before being heated for 30 min. at

70°C and centrifuged for 10 min. at 8000 g and 4 °C. The supernatant was collected and the residue was repeatedly extracted with 80% ethanol. All collected supernatants were mixed. After 30 min of incubation in a water bath at 80°C, 1 ml sample of the filtrate was mixed with 5 ml of anthrone reagent and placed in a boiling water bath. The blank consisted of 5 ml of the reagent and 2.5 ml of dist. water until the color became clear blue green, according to the method described by McCready *et al.* (1950).

Histological studies on sunflower roots under field conditions

Root segments (1–2 cm in length) were excised from the primary and lateral roots of treated sunflower plants at 10 weeks of age for histological examination. The specimens were thoroughly rinsed with dist. water and fixed in Formalin–Acetic Acid–Alcohol (FAA) solution, consisting of 85 mL of 70% ethyl alcohol, 10 mL formalin, and 5 mL glacial acetic acid. Subsequently, the samples were dehydrated through a graded series of butyl alcohol and then embedded in paraffin wax. Sections were double-stained with crystal violet and erythrosine, and cleared and mounted in Canada balsam, following the procedure reported by Farag and Shaaban (2021).

Statistical analyses

The experimental data were subjected to statistical analyses through the F-test, and differences among treatments were evaluated using the Least Significant Difference (LSD) at the 5% probability level (p value), following the methodology described by Gomez and Gomez (1984).

Results

Isolation and molecular identification of Macrophomina phaseolina

Macrophomina phaseolina was successfully isolated from 10 symptomatic sunflower samples. The colonies on PDA initially appeared white and cottony, turning dark grey to black after 7 d at 25°C. Microsclerotia were observed after 10 d, appeared as small black, round or irregular structures. Microscopic examination showed septate, hyaline hyphae with abundant microsclerotia. Specific primers were used for molecular identification of the fungal pathogen. The pair of primers produced a 350 bp fragment. The isolate was found to be a member of the species *M. phaseolina*.

Efficacy of CAPE encapsulation within the chitosan matrix

Cross-linked chitosan served as an effective matrix for the formulation of NPs, encapsulating bioactive compounds such as caffeic acid phenethyl ester (CAPE). CH-CAPE NPs were synthesized *via* the ionic gelation method, employing sodium tripolyphosphate (TPP) as a cross-linking agent. The resulting nanocomposite was characterized for its morphological features and particle size using SEM, DLS, and Zeta Sizer analysis. The efficiency of CAPE encapsulation within the chitosan matrix was evaluated through Spectroscopy FTIR with attenuated total reflectance (FTIR-ATR), and UV-Visible spectroscopy.

Characterization of CH-NPs

Visual inspection of the CH-NPs solution revealed a color change to pale white, indicating successful NPs formation. TEM further confirmed the morphology and size (51 nm) of the CH-NPs, revealing quasi-spherical and star-like clustered structures, often appearing as smaller aggregated forms. DLS analysis showed an average particle size of approximately 51 nm, while ZP measurements indicated a positive surface charge of +8.5 mV, reflecting moderate colloidal stability. X-ray diffraction (XRD) analysis displayed predominantly the amorphous nature of the CH-NPs, with broad diffraction peaks observed at 2θ values of 22.488° and 27.813°, corresponding to characteristic reflections typically associated with semi crystalline biopolymer matrices (Figure 1).

Characterization of CAPE NPs

Visual observation of the CAPE-NP suspension revealed a color change to pale yellow, indicating successful NPs formation. TEM images demonstrated well-defined and uniform particle's morphology. The NPs exhibited an average hydrodynamic diameter of approximately 78 nm, as shown in Figure 2A1, A2. ZP analysis indicated a negative surface charge of −33.45 mV (Figure 2C), suggesting good colloidal stability. The structural characteristics of the CAPE-NPs were further confirmed by XRD analysis (Figure 2D), which displayed two distinct peaks at 2θ values of 22.414° and 24.146°, corresponding to diffraction indices of 1526 and 1596, respectively, indicating the crystalline nature of the encapsulated compound within the NPs matrix.

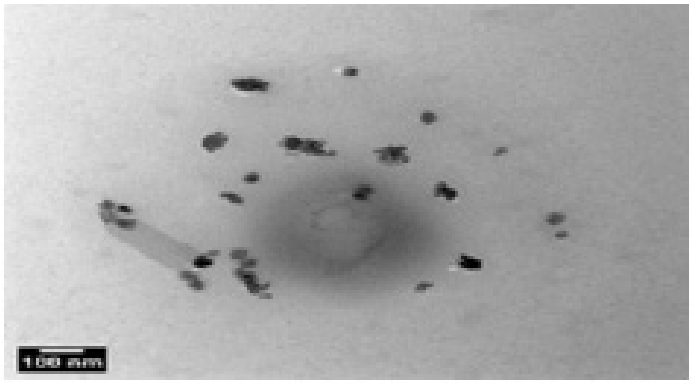

(A1) TEM of CH-NPs at 50 nm

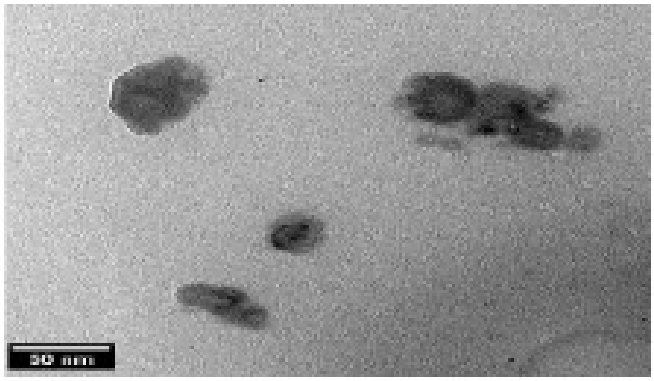

(A2) TEM of CH-NPs at 100 nm

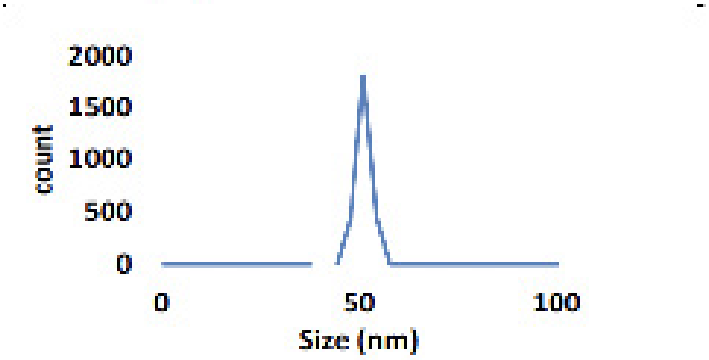

(B) Dynamic light scattering (DLS) of CH-NPs ~51

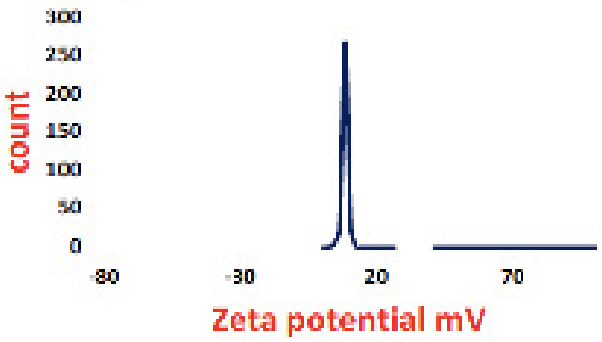

(C) Zeta potential of CH-NPs ~ 8.5 mv

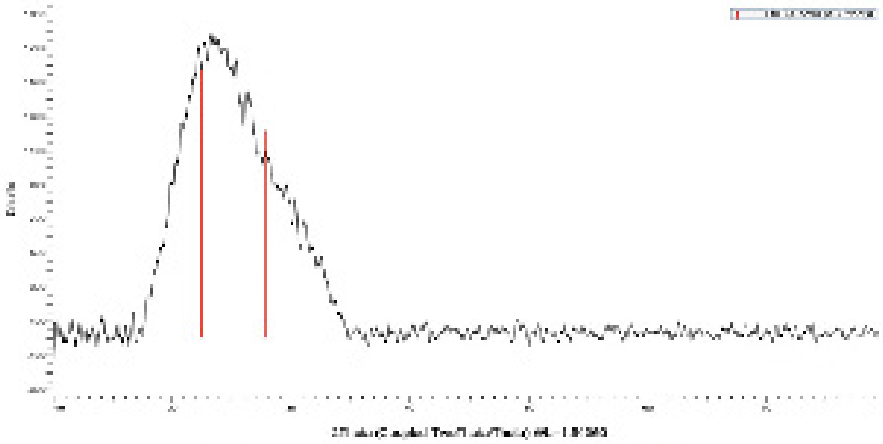

(D) X-ray diffraction (XRD) of CH-NPs

Figure 1: *Physiochemical characterization of the synthesized chitosan nanoparticles (CH-NPs).*

Characterization of CH-CAPE nanocomposite

Transmission Electron Microscopy (TEM) micrographs of the CH-CAPE- NPs revealed a uniform morphology with an average hydrodynamic size of approximately 84 nm as shown in Figure 3A, B. ZP analysis indicated a negatively charged surface, with a measured value of -18.6 mV, suggesting moderate colloidal stability (Figure 3C). The crystalline structure of the CH-CAPE- NPs was further analyzed using XRD, which exhibited multiple characteristic peaks at 2θ values of 12.246°, 14.108°, 17.781°, 21.003°, 23.625°, 24.512°, and 25.483°. These peaks corresponded to diffraction indices of 607, 3247, 1703, 1637, 1122, 847, and 769, respectively, indicating a semi-crystalline nature of the nanocomposite with distinct structural features.

Effect of different concentrations of bulk, nanoparticles, and composite-based NPs on growth of M. phaseolina in vitro

The effects of CAPE, CH, and composite treatments; along with their nanoformulations CAPE-NPs, CH-NPs, and CH-CAPE nanocomposite on the *in vitro* mycelial growth of the *M. phaseolina* were evaluated on PDA across three tested concentrations (*i.e.*, 50, 100, and 200 µg/ml) (Figure 4). Mycelial growth diameter

Links Researchers

was measured after incubation, and growth inhibition was calculated relative to the untreated control, which showed full fungal development recording a diameter of 8.2 cm.

The CAPE-NPs treatment at 100 and 200 µg/ml achieved complete (100%) inhibition of mycelial growth. Notably, even at 50 µg/ml, CAPE-NPs reduced the mycelial growth by 90.2%, compared to 61.4% inhibition by the bulk CAPE at the same tested concentration. Similarly, CH-CAPE-NPs treatments demonstrated strong antifungal potential, with inhibition rates of 84.1% and 100% at 100 and 200 µg/ml, respectively. In contrast, the bulk composite showed 98% inhibition at the highest concentration (200 µg/ml) and limited inhibition (13.4%) at 50 µg/ml. Chitosan treatments presented different patterns, where increasing their concentrations were not associated with increased efficacy. While 50 µg/ml chitosan inhibited growth by 58.5%, higher concentrations resulted in reduced inhibition, recording 26.8% only at 200 µg/ml. However, CH-NPs reversed this trend and displayed a remarkable increase in efficacy with concentration achieving 99.2%

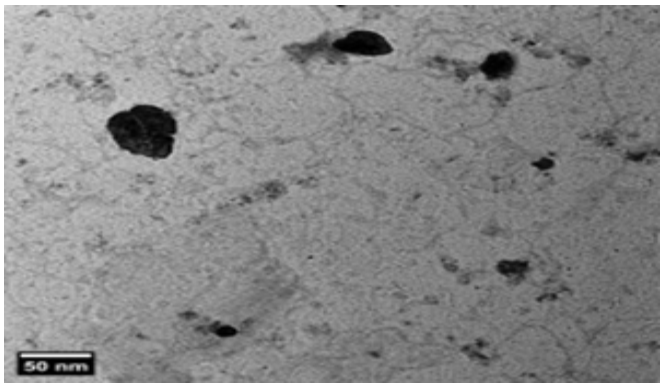

(A1) TEM of CAPE-NP at 50 nm

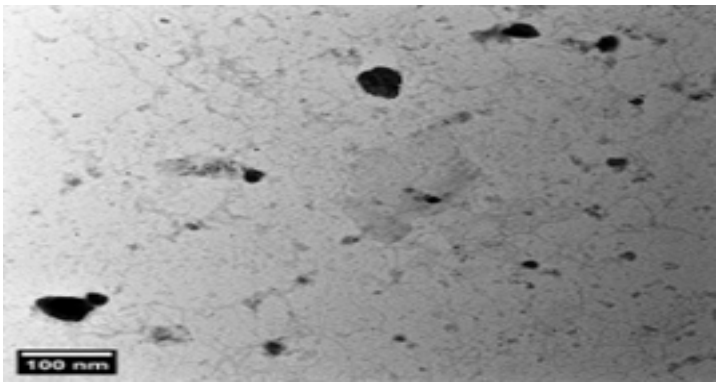

(A2) TEM of CAPE-NP at 100 nm

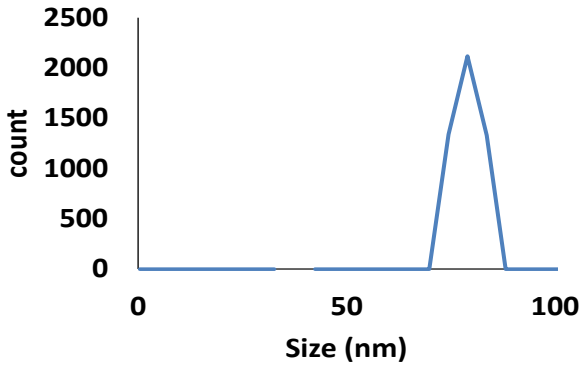

(B) DLS of CAPE-NP =78 nm

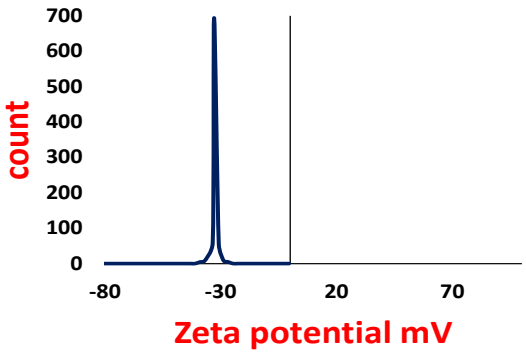

(C) Zeta potential of CAPE-NP = -33.45 mv

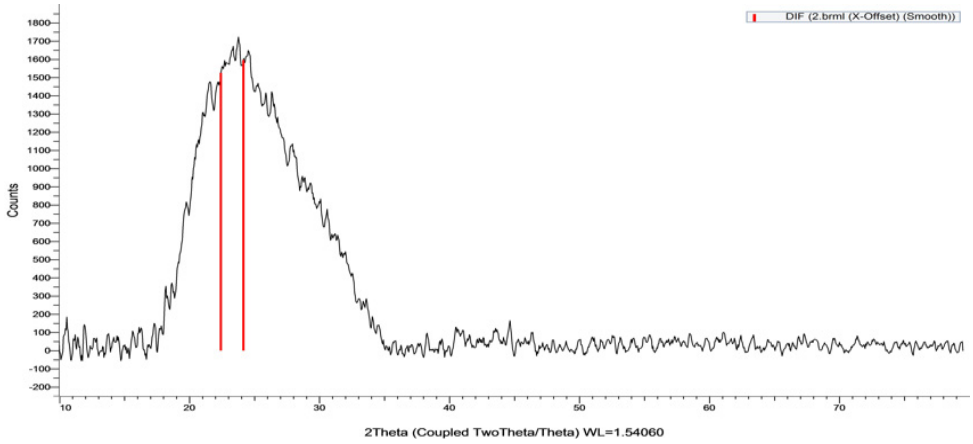

(D) XRD of CAPE-NP

Figure 2: *Physiochemical characterization of synthesized Caffeic acid phenethyl ester nanoparticles (CAPE NPs).*

Links Researchers

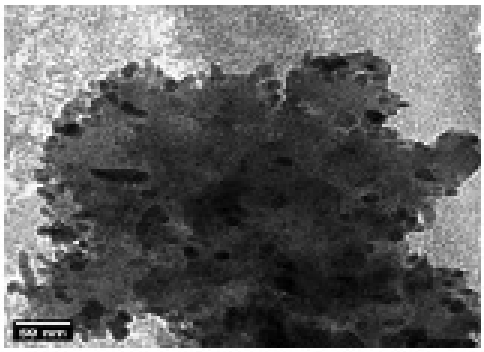

(A1) TEM of CH-CAPE- NPs at 50nm

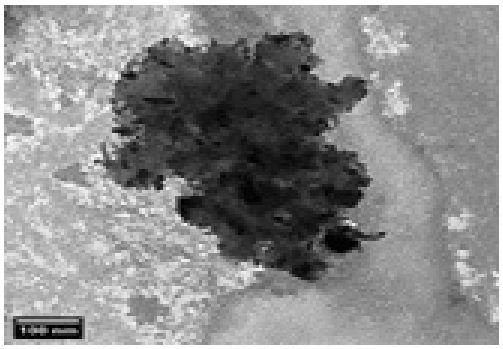

(A2) TEM of CH-CAPE- NPs at 100nm

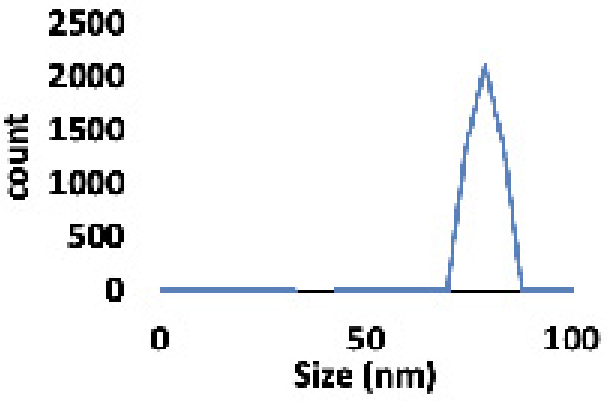

(B) Dynamic light scattering (DLS) of CH-CAPE-NPs =84nm

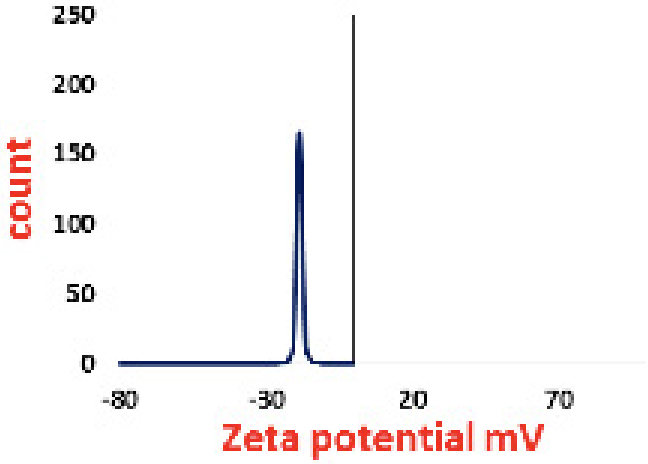

(C) Zeta potential of CH-CAPE- NPs =-18.6 mv

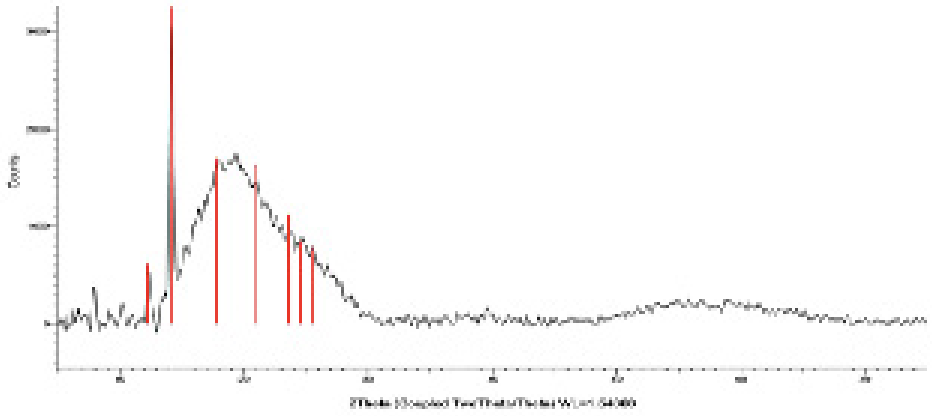

(D) X-ray diffraction (XRD) of CH-CAPE- NP

Figure 3: *Physiochemical characterization of synthesized chitosan-caffeic acid phenethyl ester (CH-CAPE) nanocomposite.*

inhibition at 200 µg/ml. These findings indicated that nanoformulations substantially enhanced antifungal efficacy across all the used treatments, with CAPE-NPs and CH-CAPE-NPs nanocomposite being the most effective.

Effect of bulk, nanoparticles, and composite-based NPs on charcoal rot incidence in sunflower under field conditions

Based on the data collected during the two successive field seasons (2023 and 2024), all applied treatments including bulk, nanoformulated compounds, and the chemical fungicide demonstrated considerable reductions in charcoal rot incidence, compared to the untreated control. The control consistently recorded the highest levels of infection, with disease incidences of 60 % and 65% in the first and second seasons,

Links Researchers

respectively.

Among the treatments, nanoformulations displayed the most pronounced suppressive effects on disease development. Plants treated with CAPE-NPs expressed the greatest reduction in charcoal rot incidence, with disease levels of 22% and 20% in the first and second seasons, respectively. These reductions corresponded to efficacy rates of 63.33% and 69.23%, remarkably exceeding the bulk form of CAPE. Nano composite (CH-CAPE-NPs) treatments also resulted in strong disease suppression, recording 24% and 23.0% disease incidences and corresponding to 60% and 64.62% efficacy across the two seasons. In contrast, bulk CH treatments were less effective, with efficacy values of 41.67% and 49.23%, while CH-NPs substantially enhanced disease suppression, reaching 26% and 24% disease incidences. The bulk composite formulation showed moderate results, achieving 50% and 57.69% efficacy, which were substantially

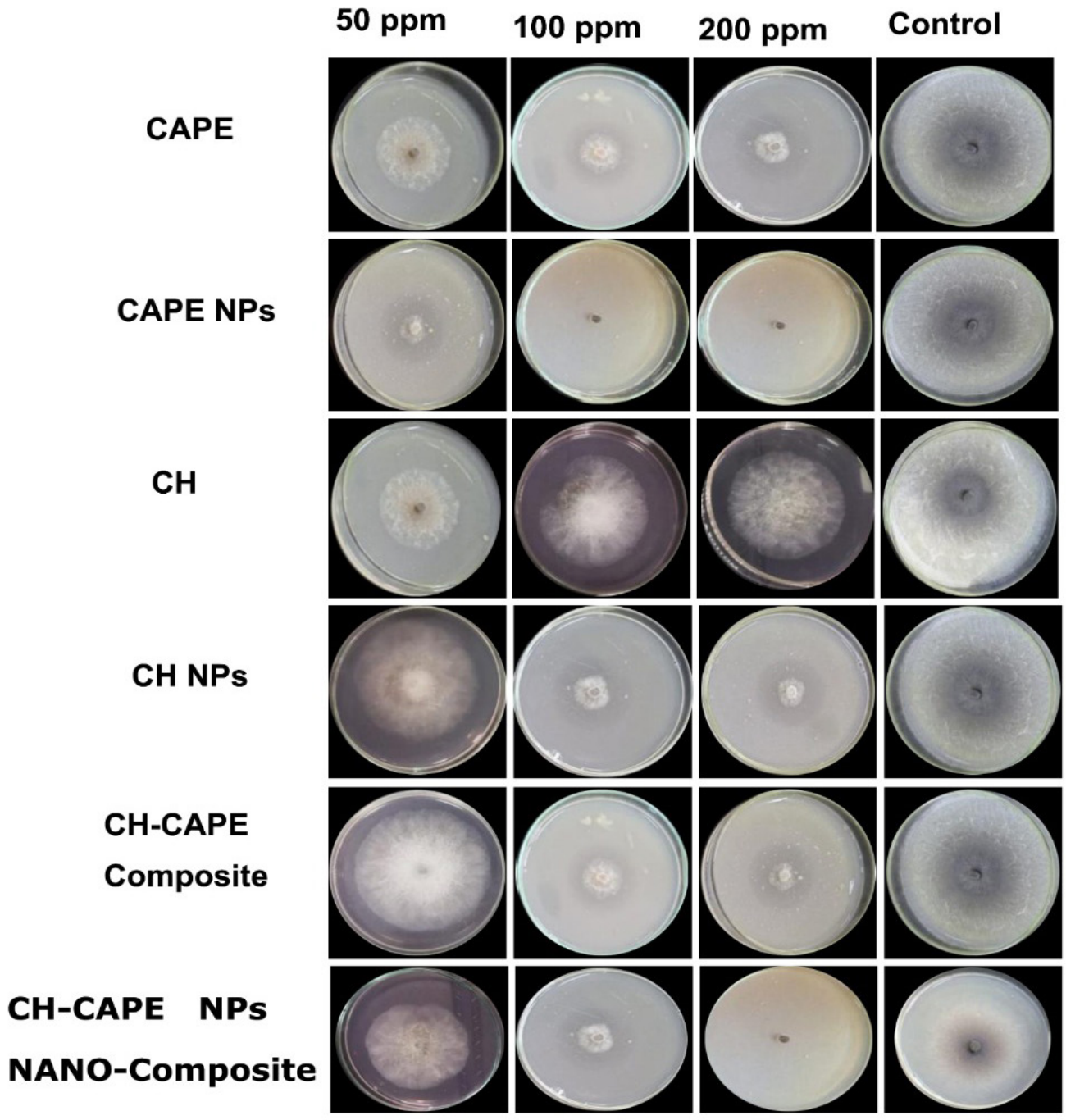

Figure 4: *Antifungal activity of Chitosan-Caffeic acid phenethyl ester nanocomposites (CH-CAPE-NPs) at different concentrations against M. phaseolina on PDA medium. Where; CAPE: caffeic acid phenethyl ester; CAPE NPs: caffeic acid phenethyl ester nanoparticles; CH: Chitosan; CH NPs: Chitosan nanoparticles; CH-CAPE composite: Chitosan - caffeic acid phenethyl ester; CH-CAPE NPs Nanocomposite: Chitosan - caffeic acid phenethyl ester nanocomposites.*

Links Researchers

improved by its nanoformulated counterpart. Notably, treatment with the Rizolex-T50 fungicide recorded the highest overall control efficiency, with disease incidences reduced to 18% and 14.1%, corresponding to efficacy rates of 70% and 78% in the first and second seasons, respectively (Table 1).

Effect of bulk, nanoparticles, and composite-based NPs on sunflower yield under field conditions

The influence of various treatments including bulk and nanoformulated CAPE, CH, CH-CAPE composite treatments, and the chemical fungicide on sunflower yield was evaluated across two consecutive growing seasons (2023 and 2024).

In both seasons, the untreated control recorded the lowest yield and 1000-seed weight values, recording 920 kg and 750 kg, and seed weights of 50.4 g and 49.4 g in the two seasons 2023 and 2024, respectively (Table 2). Among the tested treatments, CAPE-NPs achieved the highest yield improvements, recording 1510 kg in 2023 and 1325 kg in 2024. These values corresponded to yield increases of 64.13 and 76.67%, respectively, compared to the control. In terms of seed quality, CAPE-NPs also produced the heaviest seeds, with 1000-seed weights of 70.4 g (2023) and 79.2 g (2024), marking 39.68 % and 60.36 % increases, respectively. Similarly, Nano composite CH-CAPE-NPs considerably enhanced yield and seed weight across both seasons, with respective yield increases of 60.87 %, and 73.33 % and 1000-seed weight improvements of 35.32% and 42.51%, respectively.

Table 1: *Effect of bulk, nanoparticles, and composite-based NPs on charcoal rot Incidence in sunflower under field conditions across two growing seasons (2023 and 2024).*

Treatments	First season 2023		Second season 2024	
	Charcoal rot %	Efficacy %	Charcoal rot %	Efficacy %
CAPE	28.4 ± 0.18 **	52.67	30.2 ± 0.04**	53.54
CAPE NPs	22 ± 0.21**	63.33	20 ± 0.16**	69.23
CH	35 ± 0.30**	41.67	33 ± 0.45**	49.23
CH NPs	26 ± 0.25**	56.67	24 ± 0.28**	63.08
CH-CAPE composite	30 ± 0.22**	50.00	27.5 ± 0.05**	57.69
CH-CAPE NPs Nanocomposite	24 ± 0.17**	60.00	23 ± 0.19**	64.62
Fungicide (Rizolex-T50)	18 ± 0.26**	70.00	14.1 ± 0.18**	78.31
Control	60 ± 0.25	0.00	65 ± 0.20	0.00

*Where; CAPE: caffeic acid phenethyl ester; CAPE NPs: caffeic acid phenethyl ester nanoparticles; CH: Chitosan; CH NPs: Chitosan nanoparticles; CH-CAPE composite: Chitosan-caffeic acid phenethyl ester; CH-CAPE NPs Nanocomposite: Chitosan-caffeic acid phenethyl ester nanocomposites. Data are expressed as mean± SE for Gaussian variables. **The mean difference is significant compared to the control (p< 0.01).*

Table 2: *Effect of bulk, nanoparticles, and composite-based NPs on sunflower yield in two growing seasons (2023 and 2024).*

Treatments	First season (2023)				Second season (2024)			
	1000 seed weight (g)	Increase %	Yield (kg/ feddan)	Increase %	1000 seed weight (g)	Increase %	Yield (kg/ feddan)	Increase %
CAPE	62 ± 0.2**	23.02	1120 ± 0**	21.74	62.3 ± 0.06**	26.11	910 ± 0.99**	21.33
CAPE NPs	70.4 ± 0.04**	39.68	1510 ± 0.9**	64.13	79.2 ± 0.06**	60.32	1325 ± 0**	76.67
CH	61.2 ± 0.04*	21.43	1080 ± 0.4*	17.39	62.9 ± 0.02*	27.33	900 ± 0.6*	20.00
CH NPs	63 ± 0.2**	25.00	1160 ± 0.6**	26.09	68.2 ± 0.06**	38.06	1220 ± 0.9**	62.67
CH-CAPE composite	62.8 ± 0.06*	24.60	1120± 0.9**	21.74	65.3 ± 0.14*	32.19	990 ± 0.98**	32.00
CH-CAPE NPs Nanocomposite	68.2 ± 0.04**	35.32	1480 ± 0.8**	60.87	70.4 ± 0.02**	42.51	1300 ± 0.6**	73.33
Fungicide (Rizolex-T50)	57 ± 0.06*	13.10	1060 ± 0.99*	15.22	59.8 ± 0.04**	21.05	930 ± 0.6*	24.00
Control	50.4 ± 0.09	0	920 ± 0.9	0	49.4 ± 0.06	0	750 ± 0.9	0

*Where; CAPE: caffeic acid phenethyl ester; CAPE NPs: caffeic acid phenethyl ester nanoparticles; CH: Chitosan; CH NPs: Chitosan nanoparticles; CH-CAPE composite: Chitosan - caffeic acid phenethyl ester; CH-CAPE NPs Nanocomposite: Chitosan - caffeic acid phenethyl ester nanocomposites. Data are expressed as mean± SE for Gaussian variables. *The mean difference is significant as compared to the control (p< 0.01). **The mean difference is significant as compared to the control (p< 0.001).*

Links Researchers

Table 3: *Effect of bulk, nanoparticles, and composite-based NPs on the vegetative growth characteristics of sunflower under field conditions during 2023 growing season.*

Treatments	Plant height (cm)			Plant weight (g)			Head diameter (cm)
	Shoot length (cm)	Root length (cm)	Total plant height (cm)	Shoot weight (g)	Root weight (g)	Total plant weight (g)	
CAPE	195 ± 0.06**	20.7 ± 0.06**	216 ± 0.02**	910 ± 0.08**	198.1 ± .012**	1108.3 ± 0.08**	11.4 ± 0.08**
CAPE NPs	271 ± 0.02**	33 ± 0.04**	304 ± 0.1**	1280 ± 0.0**	510 ± 0.12**	1790.2 ± 0.06**	18.64 ± 0.1**
CH	220.7 ± 0.06**	19.3 ± 0.08**	240.3 ± 0.04**	870 ± 0.14**	163.2 ± 0.12**	1033 ± 0.02**	10.9 ± 0.12
CH NPs	225 ± 0.06**	23.2 ± 0.06**	248.2 ± 0.08**	1200 ± 0.18**	310.4 ± 0.08**	1510.4 ± 0 .04**	14.3 ± 0.12**
CH-CAPE composite	222.1 ± 0.1**	21 ± 0.14**	243 ± 0.1**	930 ± 0.2**	287.5 ± 0.04**	1217 ± 0.02**	13.2 ± 0.06*
CH-CAPE NPs Nanocomposite	240.5 ± 0.08**	28.2 ± 0.08**	268.7 ± 0.04**	1130 ± 0.12**	490.2 ± 0.02**	1620.2 ± 0.04**	16.41 ± 0.04**
Fungicide (Rizolex-T50)	198 ± 0.04*	17.8 ± 0.08*	215 ± 0.08**	760 ± 0.16**	160 ± 0.08	920 ± 0.02**	9 ± 0.04
Control	145 ± 0.12	13.7 ± 0.06	158.8 ± 0.02	480 ± 0.06	110 ± 0.12	590 ± 0.07	8±0.08

*Where; CAPE: caffeic acid phenethyl ester; CAPE NPs: caffeic acid phenethyl ester nanoparticles; CH: Chitosan; CH NPs: Chitosan nanoparticles; CH-CAPE composite: Chitosan – caffeic acid phenethyl ester; CH-CAPE NPs Nanocomposite: Chitosan – caffeic acid phenethyl ester nanocomposites. Data are expressed as mean± SE for Gaussian variables. *The mean difference is significant as compared to the control (p< 0.01). **The mean difference is significant as compared to the control (p< 0.001).*

Table 4: *Effect of bulk, nanoparticles, and composite-based NPs on the vegetative growth characteristics of sunflower under field conditions during 2024 growing season.*

Treatments	Plant height (cm)			Plant weight (g)			Head diameter (cm)
	Shoot length (cm)	Root length (cm)	Total plant height (cm)	Shoot weight (g)	Root weight (g)	Total plant weight (g)	
CAPE	199.8 ± 0.12**	21.3 ± 0.04**	221.1 ± 0.12**	950 ± 0.12**	171.7 ± 0.02**	1121.7 ± 0.06**	12.4 ± 0.14**
CAPE NPs	280.1 ± 0.04**	29 ± 0.14**	309.1 ± .01**	1210 ± 0.0**	460 ± 0.12**	1670 ± 0.04**	17.1 ± 0.16**
CH	191.5 ± 0.04**	20.7 ± 0.04**	212.2 ± 0.04**	800 ± 0.14**	154.2 ± 0.12**	954.2 ± 0.02**	11.9 ± 0.12
CH NPs	228 ± 0.06**	21.7±0.01**	249.7 ± 0.03**	1110 ± 0.18**	206.5 ± 0.08**	1316.5 ± 0.04**	13.8 ± 0.12**
CH-CAPE composite	212 ± 0.0**	25 ± 0.14**	237 ± 0.1**	1000 ± 0.2**	175.3 ± 0.04**	1175.3 ± 0.02**	13.3 ± 0.06*
CH-CAPE NPs nanocomposite	236.7 ± 0.08**	26.5 ± 0.68**	263.2 ± 0 .04**	1150 ± 0.12**	453.3 ± 0.02**	1603.3 ± 0.04**	14.2 ± 0.04**
Fungicide (Rizolex-T50)	190 ± 0.14*	19 ± 0.08*	209 ±. 008**	700 ± 0.16**	109.2 ± 0.08	809.2 ± 0.02**	11.3 ± 0.04
Control	132.2 ± 0.1	17 ± 0.1	149.2 ± 0.14	400 ± 0.06	108 ± 0.12	508 ± 0.07	11.2 ± 0.06

*Where; CAPE: caffeic acid phenethyl ester; CAPE NPs: caffeic acid phenethyl ester nanoparticles; CH: Chitosan; CH NPs: Chitosan nanoparticles; CH-CAPE composite: Chitosan – caffeic acid phenethyl ester; CH-CAPE NPs Nanocomposite: Chitosan – caffeic acid phenethyl ester nanocomposites. Data are expressed as mean± SE for Gaussian variables. *The mean difference is significant as compared to the control (p<0.01). **The mean difference is significant as compared to the control (p< 0.001).*

CH-NPs provided moderate improvements in both parameters, exceeding its bulk form. In contrast, bulk CH and composite treatments showed moderate to low efficacy in increasing sunflower yield. Interestingly, the chemical fungicide (Rizolex-T50) expressed relatively lower improvements in both yield and seed weight compared to CAPE-NPs and nano composite (CH-CAPE-NPs). Yield improvements with the fungicide were 15.22 % and 24.00 %, while seed weight increases were 13.10 % and 21.05 % in both seasons 2023 and 2024, respectively. These results underscore the superior effectiveness of nanoformulations, especially CAPE-NPs and nano composite (CH-CAPE-NPs) in enhancing both productivity and seed quality under field conditions, compared to the bulk treatments and the chemical fungicide.

Effect of bulk, nanoparticles, and composite-based NPs on the vegetative growth characteristics of sunflower under field conditions

In the average data across the two growing seasons 2023 and 2024, various treatments particularly their nanoformulations remarkably improved sunflower vegetative growth parameters compared to the untreated control (Tables 3 and 4). Among all treatments, CAPE-NPs consistently produced

the most pronounced enhancements in plant development, including plant height, total plant weight, head diameter, and shoot and root biomass under field conditions. CAPE-NPs treatments exhibited the tallest shoot recording 271 cm, the highest total plant weight of 1790.2 g, and the greatest head diameter of 18.64 cm, with substantial increases across all the measured parameters, compared to both the bulk CAPE and the untreated controls. Similarly, nanocomposite CH-CAPE-NPs treatments ranked second in performance, considerably boosting all vegetative growth traits, including shoot and root weights, which reached an average of 1130 g and 490.2 g, respectively. These were accompanied with a substantial improvement in head diameter, recording an average of 16.41 cm, indicating enhanced reproductive development. The impact of CH-NPs was also notable, particularly in shoot (225 cm) and root (23.2 cm) development, total plant weight averaging 1510.4 g, and head size of 14.3 cm, outperforming its bulk counterpart (CH), which showed only modest gains. In contrast, treatments with bulk CH and CH-CAPE composite formulations displayed moderate increases in plant growth parameters, with lower plant height, biomass, and head diameter compared to their nanoforms. The fungicide (Rizolex-T50) treatment reduced disease incidence, but recorded the lowest vegetative growth improvements among the treated plants, indicating its limited benefit to growth promotion. As expected, the control group under filed conditions displayed the poorest performance, with considerably reduced plant height average (158.8 cm), lowest total plant weight (590 g), and minimal head diameter of 8 cm. The second season also exhibited a comparable trend.

Effects of bulk, nanoparticles, and composite-based NPs on conjugated, free, and total phenolic contents in sunflower

Data in Table 5 indicated that in both seasons, the CAPE-NPs treatment consistently exhibited the highest increases in all phenolic content parameters, compared to the control and the other treatments. In the first season (2023), CAPE-NPs recorded 22.10 mg/g of free phenol, 67.05 mg/g ofconjugated phenol, and 155.26 % increase in total phenol. This was closely followed by the nanocomposite CH-CAPE-NPs treatment, which also showed remarkable improvements, with 109.35 % increase in total phenol. Similarly, in the second season (2024), CAPE-NPs expressed substantial increases in total phenol by 168.35 % increase. Nanocomposite CH-CAPE-NPs also performed well recording 20.89 mg/g, 53.6 mg/g, and 74.44 mg/g in free, conjugated, and total phenol, respectively, corresponding to increases of 125.07 % in total phenol compared to the control.

Treatments with CH and CH-NPs caused moderate enhancements in phenolic content, with CH-NPs being superior to bulk CH. The composite CH-CAPE treatment also displayed some improvement, although less pronounced compared to its nano form. Meanwhile, the fungicide and the control treatments recorded the lowest values across all the tested phenolic parameters in both seasons,

Influence of bulk, nanoparticles, and composite-based NPs on the carbohydrate contents in sunflower

The obtained results presented in Figures 5, 6 clearly demonstrated that application of the CAPE-NPs and nanocomposite CH-CAPE-NPs treatments considerably enhanced the accumulation of sugars in sunflower, particularly the reduced and total sugar contents. Compared to the fungicide and the control, all nano-based treatments resulted in a marked increase in sugar levels, where CAPE-NPs showed the most pronounced effect. This enhancement was consistent across both growing seasons 2023 and 2024.

Effects of bulk, nanoparticles, and composite-based NPs on oxidative enzymes activity in sunflower

The data presented in Table 6 revealed that application of NPs-based treatments appreciably enhanced the activity of the defense-related enzymes in sunflower, mainly POD, PPO, and CAT, across both the 2023 and 2024 growing seasons.

The data obtained showed that all treatments enhanced the activity of these enzymes compared to the untreated control in both growing seasons. CAPE-NPs significantly elevated the enzymatic activities in sunflower, with POD reaching 5.25 U/g and 5.71 U/g, PPO 1.4 U/g and 1.54 U/g, and CAT 2.15 U/g and 2.34 U/g during the first and second seasons, respectively, compared to the control showing POD of 1.89 U/g, PPO of 0.80 U/g, and CAT of 0.77 U/g in the first season and POD 1.99 U/g, PPO 0.88 U/g, and CAT 0.65 U/g in the second season.

Table 5: *Effects of bulk, nanoparticles, and composite-based NPs on conjugated, free, and total phenolic content over two consecutive growing seasons (2023 and 2024).*

Treatments	First season (2023)				Second season (2024)			
	Free phenolic contents (mg/g)	Conjugated phenolic contents (mg/g)	Total phenolic contents (mg/g)	Increase %	Free phenolic contents (mg/g)	Conjugated phenolic contents (mg/g)	Total phenolic contents (mg/g)	Increase %
CAPE	19.79 ± 0.01**	26.68 ± 0.03**	46.47 ± 0.02**	33.05	15.68 ± 0.01**	31 ± 0.1**	46.67 ± 0.01**	41.27
CAPE NPs	22.10 ± 0.02**	67.05 ± 0.01**	89.15 ± 0.03**	155.26	21.89± 0.01**	67 ± 0.08**	88.80 ± 0.0**	168.53
CH	16.14 ± 0.008*	22.01 ± 0.02*	38.15 ± 0.03*	9.22	14.99 ± 0.01*	22.8 ± 0.04*	37.75 ± 0.03*	14.21
CH NPs	20.34 ± 0.03**	35.54 ± 0.03**	55.88 ± 0.02**	59.96	16.11 ± 0.01**	40.8 ±. 004**	56.94 ± 0.01**	72.33
CH-CAPE composite	17.66 ± 0.02*	26.13 ± 0.0*	43.79 ± 0.01*	25.37	15.53 ± 0.02*	28.15 ± 0.03*	43.68 ± 0.03*	32.14
CH-CAPE NPs Nanocomposite	21.66 ± 0.02**	51.46 ± 0.08**	73.12 ± 0.03**	109.35	20.89 ± 0.02**	53.6 ± .002**	74.44 ± 0.11**	125.07
Fungicide (Rizolex-T50)	14.99 ± 0.01	21.5 ± 0.02	36.49 ± 0.04*	4.47	14.27 ± 0.03*	19.5 ± 0.04	33.75 ± 0.01	2.11
Control	13.8 ± 0.16	21 ± 0.2	34.93 ± 0.06	0	13.84 ± 0.01	19.5 ± 0.1	33.06 ± 0.01	0

Where; CAPE: caffeic acid phenethyl ester; CAPE NPs: caffeic acid phenethyl ester nanoparticles; CH: Chitosan; CH NPs: Chitosan nanoparticles; CH-CAPE composite: Chitosan - caffeic acid phenethyl ester; CH-CAPE NPs Nanocomposite: Chitosan - caffeic acid phenethyl ester nanocomposites. Data are expressed as mean± SE for Gaussian variables. *The mean difference is significant as compared to the control (p<0.01). **The mean difference is significant as compared to the control (p< 0.001).

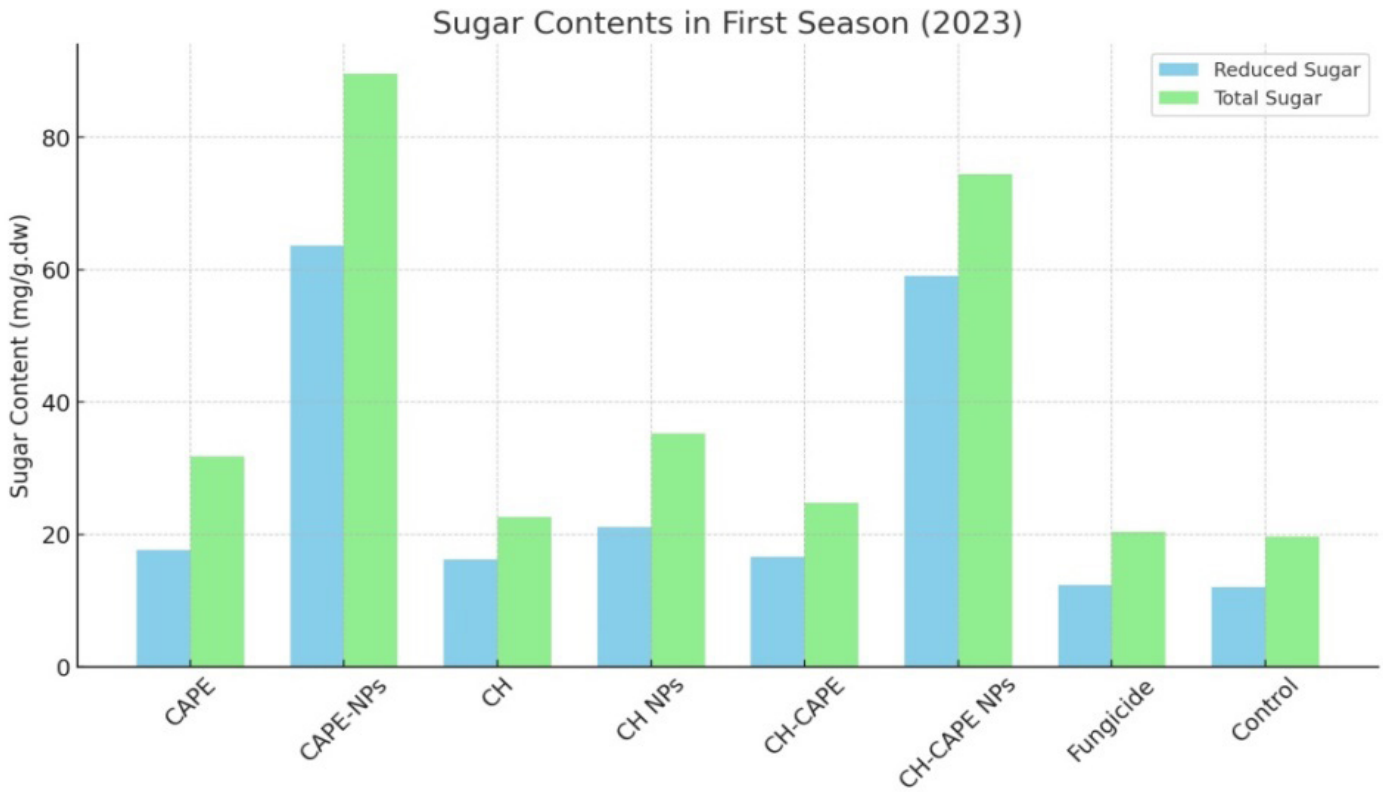

Figure 5: *Influence of nanoparticles and nanocomposite on the carbohydrate contents, including reducing sugars and total carbohydrates during the 2023 growing season. Where; CAPE: caffeic acid phenethyl ester; CAPE NPs: caffeic acid phenethyl ester nanoparticles; CH: Chitosan; CH NPs: Chitosan nanoparticles; CH-CAPE composite: Chitosan - caffeic acid phenethyl ester; CH-CAPE NPs Nanocomposite: Chitosan - caffeic acid phenethyl ester nanocomposites.*

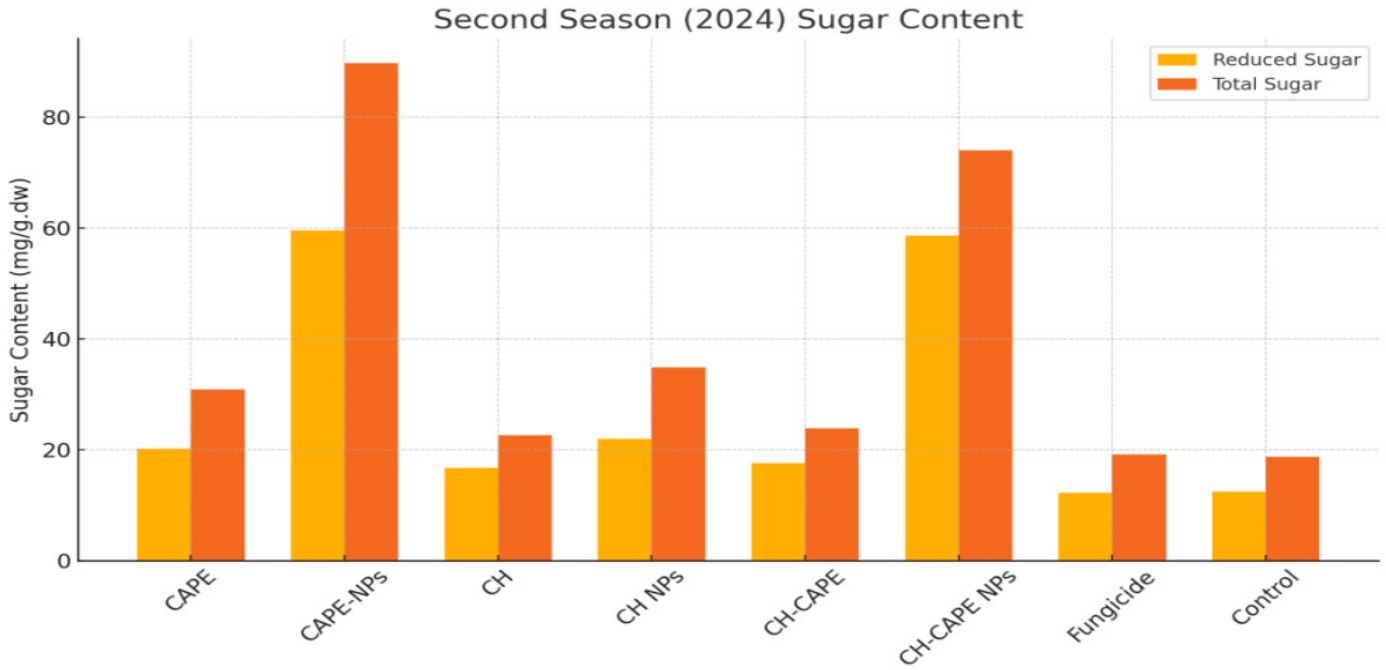

Figure 6: *Influence of nanoparticles and nanocomposite on the carbohydrate contents, including reducing sugars and total carbohydrates during the 2024 growing season. Where; CAPE: caffeic acid phenethyl ester; CAPE NPs: caffeic acid phenethyl ester nanoparticles; CH: Chitosan; CH NPs: Chitosan nanoparticles; CH-CAPE composite: Chitosan - caffeic acid phenethyl ester; CH-CAPE NPs Nanocomposite: Chitosan - caffeic acid phenethyl ester nanocomposites.*

Table 6: *Effects of bulk, nanoparticles, and composite-based on oxidative enzymes activities over two consecutive growing seasons (2023 and 2024).*

Treatments	First season (2023)			Second season (2024)		
	POD (U/g)	PPO (U/g)	CAT (U/g)	POD (U/g)	PPO (U/g)	CAT (U/g)
CAPE	3.26 ± 0.01**	1.0 ±0 .01*	1.53 ± .002**	3.57 ±.004**	1.28 ± .008**	1.42 ± .008**
CAPE NPs	5.25 ±0 .07**	1.4 ±0 .01**	2.15 ± .004**	5.71 ±.004**	1.54 ± .004**	2.34 ± .02**
CH	2.31 ±0 .01**	0.85 ±0 .01	1.19 ± .008**	2.49 ±.01**	0.92 ± .03*	1.20 ± .02**
CH NPs	3.46 ±0 .04**	1.22 ±0 .02**	1.88 ± .008**	3.82 ±.004**	1.14 ± .01**	1.87 ± .01**
CH-CAPE composite	2.82 ±0 .01**	0.9 ±0 .04**	1.36 ± .008	3.07 ±.02*	0.97 ±. 006*	1.27 ± .05**
CH-CAPE NPs Nanocomposite	4.26 ±0 .05**	1.3 ±0 .06**	1.97 ± .006**	4.72 ± .05**	1.44 ± .01**	1.98 ± .04**
Fungicide (Rizolex-T50)	1.9 ±0 .02	0.81 ±0 .03	0.9 ± .02**	2.0 ± .04	0.9 ±. 02	0.8 ± .02**
Control	1.89 ±0 .02	0.80 ±0 .02	0.77 ± .006	1.99 ±.002	0.88 ±. 004	0.65 ± .004

*Where; CAPE: caffeic acid phenethyl ester; CAPE NPs: caffeic acid phenethyl ester nanoparticles; CH: Chitosan; CH NPs: Chitosan nanoparticles; CH-CAPE composite: Chitosan - caffeic acid phenethyl ester; CH-CAPE NPs Nanocomposite: Chitosan - caffeic acid phenethyl ester nanocomposites. Data are expressed as mean± SE for Gaussian variables. *The mean difference is significant as compared to the control (p<0.01). **The mean difference is significant as compared to the control (p< 0.001).*

Similarly, treatments with CH-CAPE NPs nanocomposite and CH NPs notably increased the enzyme activities, while bulk treatments with CH and CH-CAPE composite induced moderate enhancement. In contrast, the chemical fungicide exhibited only slight increases in enzymatic activity, with POD of 1.9 U/g, PPO of 0.81 U/g, and CAT of 0.9 U/g in the first season, and POD of 2.0 U/g, PPO of 0.9 U/g, and CAT of 0.8 U/g in the second season. Generally, the nanoformulated treatments substantially stimulated the antioxidant defense system in sunflower, likely contributing to enhanced plant resistance and growth, whereas bulk treatments and fungicide showed limited effects. A similar trend was observed in the second season indicating the reproducibility and consistency of the stimulatory effects of the tested treatments.

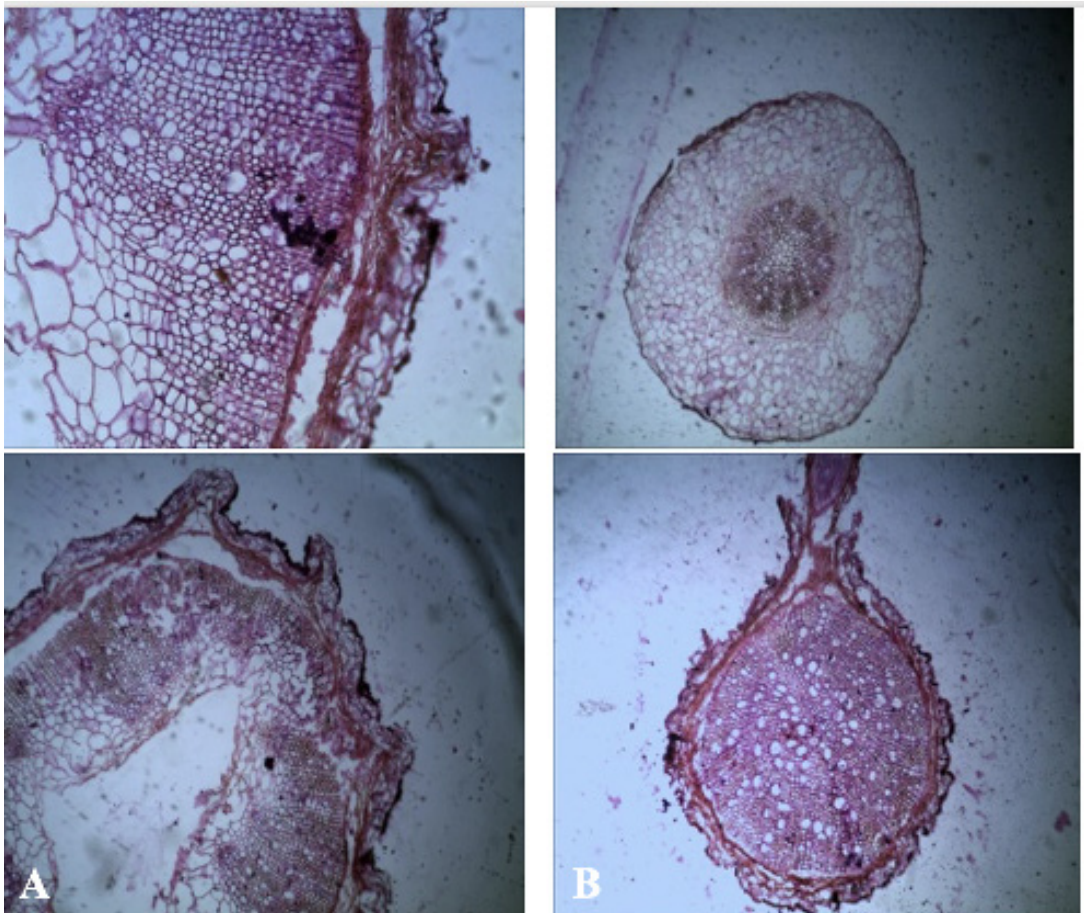

Figure 7. *Transverse sections of sunflower primary roots showing anatomical responses under treatments: (A) Control root (B) Root treated with CAPE NPs*

Anatomical structure of sunflower roots under field conditions

Microscopic examination of transverse sections of primary sunflower roots revealed appreciable histological alterations associated with the applied treatments. The results demonstrated that all treatments promoted an increase in root cross-sectional thickness compared to the untreated control. The most pronounced increase was observed in roots treated with CAPE NPs, primarily due to the expansion of both the cortex and vascular cylinder tissues. In addition, the xylem vessel diameter was markedly enlarged compared to the control. In contrast, infected control roots exhibited severe pathological changes, including the formation of mycelial masses, sclerenchymatous tissue, and intracellular pycnidia, which collectively caused deformation and destruction of the epidermal cells, and cell plasmolysis. Additional pathological features included epidermal cell swelling (tylosis), xylem vessel blockage (gummosis), and necrotic zones surrounding the xylem, often appearing as black clusters. Wide, hollow pith was also observed in these control roots. On the other hand, CAPE NPs-treated roots exhibited well-preserved anatomical features, with no disease signs (Figure 7).

Discussion

Control of fungal root diseases remains one of the most pressing challenges in food crop production globally. Among these diseases, charcoal rot caused by *M. phaseolina* is especially destructive to sunflower crops, resulting in significant yield reductions during key developmental stages. The overuse and indiscriminate application of synthetic fungicides have contributed not only to environmental pollution but also to emergence of fungicide-resistant strains of the phytopathogenic fungi.

To address these concerns, nanotechnology has emerged as a promising tool in plant pathology. Nanoparticles exhibit a broad spectrum of antimicrobial activity due to their high surface area to volume ratio and reactive properties (Kumar *et al.*, 2022). Natural and biodegradable NPs-based treatments such as CH, CAPE, and their composites have shown effectiveness in controlling soil-borne pathogens with minimal environmental impact (Liu *et al.*, 2023). Nanoformulations were synthesized

and characterized using SEM and ZP analysis. The CAPE-CH-NPs nanocomposite was prepared *via* ionotropic gelation using TPP as a crosslinking agent, and structural confirmation was achieved through FTIR and UV-Vis analyses.

In vitro antifungal assays revealed that CAPE-NPs at 100 µg/ml exhibited complete (100%) growth inhibition of *M. phaseolina*, outperforming the nanocomposite (85%) and CH-NPs (80%). This recorded high level of antifungal activity is consistent with previous findings on the efficacy of phenolic acid-based NPs (Mendes *et al*., 2022). The superior performance of CAPE-NPs can be attributed to its nanoscale formulation, which increased its surface area and enhanced the bioavailability of the active compound. NPs are effectively able to penetrate fungal cell walls, disrupt cellular structures, increase membrane permeability, and cause leakage of cellular contents, ultimately leading to cell death (Liu *et al*., 2023). Furthermore, encapsulating CAPE within chitosan contributed to a synergistic effect, as CH itself possesses inherent antimicrobial properties that further suppressed the fungal growth (Gupta *et al*., 2024).

Field experiments conducted in Giza Governorate across the 2023 and 2024 growing seasons validated these findings. CAPE-NPs yielded the highest values for growth parameters such as plant height, head diameter, 1000-seed weight, and overall seed yield. These outcomes support the findings obtained by Ibrahim *et al*. (2021), who reported improved grapevine productivity following caffeic acid application, and extended the utility of such treatments to oilseed crops like sunflower. Furthermore, the findings of recent studies also confirmed the beneficial effect of caffeic acid-based nanomaterials in the control of plant growth. Ramzan *et al*. (2024) revealed that the use of caffeic acid enhanced the plant growth characteristics, chlorophyll level, and biomass development in potato growing under stress, since caffeic acid has a wide-range of activity as a growth-regulator in crop species. Moreover, Danish *et al*. (2024) demonstrated that the use of caffeic acid with the NPs as fertilizers appreciably promoted the length of the stem, the biomass of the shoot, and the leaf development, which proves the effectiveness of the nano-assisted delivery of caffeic acid to the plants.

Nanoformulations considerably enhanced the efficacy of CAPE by improving its bioavailability, stability, and ability to activate plant defense responses. In its natural form, CAPE is poorly water-soluble, limiting its uptake by plant tissues; however, nanoscale increases its solubility, absorption, and translocation within the plant vascular systems (Kumar *et al*., 2020). Nanoscale carriers also enable targeted delivery and improved cellular penetration, allowing CAPE to more effectively reach and disrupt the microbial cells while minimizing the required dose and environmental impact (Rajeevan *et al*., 2023).

The biochemical assays showed that *M. phaseolina* infection had altered several plant defense markers, including the activities of POD, PPO, and CAT, and the accumulation of phenolic and sugar components. Notably, CAPE-NPs consistently induced high biochemical responses, suggesting a strong systemic acquired resistance (SAR) inducing effect. This is supported by Nedveda *et al*. (2022), who reported increased enzymatic activity and plant growth parameter in cucumber treated with CH and hydroxycinnamic acids conjugates. Additionally, Yalouskaya *et al*. (2023) observed similar induced systemic resistance in potatoes growing under stress using CH-based elicitors. The marked increase in oxidative enzymes activity following nanomaterial treatments indicated the activation of the plant's oxidative stress; a key early defense mechanism against the microbial pathogens (Wang *et al*., 2022). These enzymes help to detoxify ROS produced during infection and contribute to cell wall reinforcement and antimicrobial compounds biosynthesis. The elevated enzyme activities in CAPE-NPs-treated plants reflected an enhanced defensive state, consistent with the role of phenolic compounds as signaling molecules in inducing plant immunity (Zhou *et al*., 2024).

Increased levels of phenolic compounds and sugars in treated plants further suggested the induction of defense pathways. Phenolics serve as antimicrobial agents and antioxidants that protect tissues from pathogen-induced oxidative damage. Sugars act not only as energy sources but also as signaling molecules that regulate defense gene expression (Hong *et al*., 2024). The CAPE-NPs and nanocomposite treatments likely stimulated secondary metabolism pathways, resulting in the accumulation of these compounds, which enhanced resistance and promoted plant strength. The increase in phenolic and sugar compounds also aligns with Danish *et al*. (2024), who

recorded that caffeic acid enhanced yield and sugar content in potatoes. These secondary metabolites play a key role in strengthening plant defense against several fungi such as *M. phaseolina* (Asad, 2022).

The enhanced efficacy of CAPE in its nanoform is largely attributed to the physicochemical advantages conferred by nanocarrier systems, optimizing the action of its bioactive functional groups. CAPE contains key functional moieties such as catechol group (3,4-dihydroxyphenyl); a conjugated α, β-unsaturated carbonyl system and an ester linkage, all contributing to its potent antioxidant, antimicrobial, and signaling properties in plants. In their nanoform, these groups become more effective due to improved solubility, stability, and bioavailability. For instance, the catechol group, naturally scavenging ROS and chelating metal ions to reduce oxidative stress, exhibits enhanced redox activity in CAPE-NPs formulations as their increased surface area allows for greater interaction with the cellular targets (Zahin *et al*., 2017). Similarly, the α, β-unsaturated carbonyl system, known for acting as a Michael acceptor; a molecule that accepts another molecule at its double bond during a Michael addition reaction and inhibits the key microbial enzymes or modulates the plant defense proteins, benefits from the targeted delivery mechanisms in the NP's formulations. This increases its local concentration at the infection site, thereby increasing its biochemical effects (Rajeevan *et al*., 2023). Notably, the current obtained results indicated that nanoformulations can reduce reliance on synthetic fungicides, contributing to safer and more sustainable crop protection strategies (Kráľová and Jampílek, 2022). This study supports the increasing consensus that integrates nanotechnology with natural bioactive compounds, representing a viable path towards ecofriendly disease management.

Microscopic examination revealed that the applied treatments remarkably improved root anatomical traits, with CAPE-NPs showing the strongest effect. The observed increase in cortical and vascular cylinder thickness, along with enlarged xylem vessels, suggested improved water and nutrients transport capacity, crucial for maintaining plant strength under stress (Shoukat *et al*., 2024). In contrast, infected control roots displayed severe pathological features, including tylosis, gummosis, necrosis, and fungal structures that disrupted the epidermal and vascular integrity. These symptoms align with typical histological responses caused by vascular fungal pathogens, obstructing the transport pathways and causing tissue collapse (Agrios, 2005). Remarkably, CAPE-NPs-treated roots showed no such signs of infection, indicating that the nanoformulation not only promoted the plant growth but also effectively inhibited the fungal penetration. This dual effect may be attributed to the strong antifungal activity and bioprotective properties of CAPE-NPs, consistent with a previous report highlighting the antimicrobial potential of NP's treatments in crops (Rai and Ingle, 2012). These results suggested that CAPE-NPs were highly effective in preventing fungal invasion while preserving root structural integrity and vascular functionality, offering a promising approach for managing soil borne pathogens and improving sunflower performance under field conditions.

Conclusions and Recommendations

The present study demonstrated the successful synthesis and characterization of chitosan-based nanocomposites incorporated with CAPE and their potential application in managing charcoal rot disease in sunflower caused by *M. phaseolina*. Among the tested formulations, CAPE-NPs exhibited the highest antifungal potential, achieving complete inhibition of pathogen growth *in vitro*. Field experiments also attested that CAPE-NPs remarkably enhanced sunflower development, yield attributes, and biochemical defense attributes, compared to the control and the additional NPs treatments. The yield was considerably improved, recording 1510 kg and 1325 kg in the year 2023 and 2024, respectively. Also, the total phenolic content was appreciably increased by 155.26%. There was also an increased antioxidant enzyme activity where the enzyme peroxidase (POD) recotded 5.25 U/g and 5.71 U/g, polyphenol oxidase (PPO) (1.4 U/g and 1.54 U/g), and catalase (CAT) (2.15 U/g and 2.34 U/g), during the first and second seasons, respectively. The accumulation of the phenolic compounds and high activities of antioxidant enzymes indicated that CAPE-NPs not just inhibited the infection of pathogens, but also triggered the systemic acquired resistance in sunflower plants. Finally, these current findings underscore CAPE-NPs as an effective, ecofriendly, and sustainable alternative to conventional fungicides for management of soil-borne fungal diseases in sunflower fields. Notably, CAPE-NPs or CAPE-CH nanocomposites have a lot of promise as a sustainable and environmentally acceptable substitute for chemical fungicides used for

the management of soil-borne fungal infections in sunflower.

Acknowledgment

The authors would like to express their sincere gratitude to the Central Laboratory for Biotechnology (CLB) at the Plant Pathology Research Institute for providing the laboratory facilities and technical support that were essential for conducting this study.

Novelty Statement

This study is the first to detail the synthesis and application of chitosan-based nanocomposites in conjunction with CAPE-NPs used in the treatment of sunflower charcoal rot disease. The work illustrates the superiority of CAPE-NPs in antifungal activity against *M. phaseolina* and in enhancing sunflower productivity, growth, and biochemical protection measures, providing a sustainable and environmentally healthy alternative to the use of the conventional chemical fungicides.

Author's Contributions

SMA: Methodology and data curation. HY: Conceptualization, investigation, writing, reviewing, editing and supervision. GMH: Reviewing, editing and supervision. RRA: Formal analysis. SSM: supervision.

Ethical approval
Not applicable.

Funding source
This study did not receive any specific funding.

Generative AI and AI assisted technology statement
The authors declare that no generative AI and AI assisted technology was used in the creation of this manuscript.

Conflict of interests
The authors have declared no conflicts of interest.

References

Aebi, H., 1974. Catalase. In: Methods of enzymatic analysis. Academic Press. pp. 673–684. https://doi.org/10.1016/B978-0-12-091302-2.50032-3

Agrios, G.N., 2005. Plant pathology, 5th ed. Elsevier Academic Press, Amsterdam/Burlington, MA, pp. 922.

Ali, M.A., Abd El Gwad, T.I., Ismail, M.E. and Galal, A.A., 2022. Eco-friendly control traits of common bean root rot caused by *Macrophomina phaseolina* and *Fusarium equiseti* using fungicide alternatives. New Valley J. Agric. Sci., 2(6): 530–543.

Asad, S.A., 2022. Mechanisms of action and biocontrol potential of Trichoderma against fungal plant diseases A review. Ecol. Complex., 49: 100978. https://doi.org/10.1016/j.ecocom.2021.100978

Bán, R., Kiss, J., Pálinkás, Z. and Körösi, K., 2023. Management of sunflower downy mildew (*Plasmopara halstedii*) under an IPM system approach. Agronomy, 13(4): 1029. https://doi.org/10.3390/agronomy13041029

Calvo, P., Remuñán-López, C., Vila-Jato, J.L. and Alonso, M.J., 1997. Chitosan nanoparticles as carriers for proteins and vaccines. Pharm. Res., 14(10): 1431–1436. https://doi.org/10.1023/A:1012128907225

Cvejić, S., Mladenov, V., Jocković, M., Krstić, M., Babec, B., Jocić, S. and Dedić, B., 2024. Sunflower genetic diversity against *Macrophomina phaseolina*. J. Agric. Sci., 30(3): 513–525.

Danish, S., Hareem, M., Imran, M., Tahir, N., Gholizadeh, F., Datta, R. and Alahmadi, T.A., 2024. Effect of caffeic acid and cobalt sulfate on potato plants. Sci. Rep., 14(1): 20663. https://doi.org/10.1038/s41598-024-70998-z

Darwesh, O.M. and Elshahawy, I.E., 2023. Management of charcoal-rot and late-wilt diseases using vermitea and wood vinegar. Sci. Rep., 13(1): 17387. https://doi.org/10.1038/s41598-023-43974-2

Dhingra, O.D. and Sinclair, J.B. 1973. Variation among isolates of *Macrophomina phaseoli* (*Rhizoctonia bataticola*) from different regions. J. Phytopathol., 76(3): 200-204.

El-Hadrami, A., Adam, L.R., El-Hadrami, I. and Daayf, F., 2010. Chitosan in plant protection. Mar. Drugs, 8(4): 968–987. https://doi.org/10.3390/md8040968

El-Rayes, M.M., Ali, I.N., Abd El-Nabi, H.M., Morsy, K.M. and Khalil, M.I., 2022. Systemic resistance in cluster bean. Egypt. J. Phytopathol., 50(2): 33–43. https://doi.

org/10.21608/ejp.2022.160238.1068

El-Wakeel, S.T., Abdel-Karim, A., Ismail, S.H. and Mohamed, G.G., 2022. Ag-dendrites-Cu nanostructure for selenium removal. Water Environ. Res., 94(4): e10713. https://doi.org/10.1002/wer.10713

Farag, H. and Shaaban, S., 2021. Botanical studies of *Lepidium sativum*. J. Plant Prod., 12(11): 1231–1240. https://doi.org/10.21608/jpp.2021.101841.1070

Farhatun Najat, M., Maluin and Hussein, M.Z., 2020. Chitosan nanoparticles in agriculture. Front. Plant Sci., 11: 1130.

Gomez, K.A. and Gomez, A.A., 1984. Statistical procedures for agricultural research. John Wiley and Sons.

Gupta, L., Kumar, P., Sen, P., Sharma, A., Kumar, L., Sengupta, A. and Vijayaraghavan, P., 2024. Bioactive molecules against *Rhizopus oryzae*. Curr. Res. Microb. Sci., 7: 100270. https://doi.org/10.1016/j.crmicr.2024.100270

Hong, P., Zhang, Z., Zhou, Y., Lu, X., Sadeghnezhad, E., Pang, Q. and Jia, H., 2024. Strawberry resistance to *Botrytis cinerea*. Sci. Hortic., 327: 112850. https://doi.org/10.1016/j.scienta.2024.112850

Ibrahim, R.E., El-Akad, M.M. and Rizkalla, M.K., 2021. Gibberellic and caffeic acids on grape yield. SVU-Int. J. Agric. Sci., 3(4): 132–140. https://doi.org/10.21608/svuijas.2021.91791.1139

Ismail, S.H., Hamdy, A., Ismail, T.A., Mahboub, H.H., Mahmoud, W.H. and Daoush, W.M., 2021. Carbopol/ZnO nanoparticles gel. Crystals, 11(9): 1092. https://doi.org/10.3390/cryst11091092

Karibasappa, C.S., Bhat, B.N. and Rao, S.C., 2020. Fungicides against *Macrophomina phaseolina*. Int. J. Curr. Microbiol. Appl. Sci., 9(4): 1293–1299. https://doi.org/10.20546/ijcmas.2020.904.152

Kolenčík, M., Ernst, D., Urík, M., Ďurišová, Ľ., Bujdoš, M., Šebesta, M. and Kratošová, G., 2020. Nanoparticles in sunflower. Nanomaterials, 10(8): 1619. https://doi.org/10.3390/nano10081619

Kráľová, K. and Jampílek, J., 2022. Nanofertilizers and nanopesticides. In: Inorganic nanopesticides and nanofertilizers, Springer. pp. 295–361. https://doi.org/10.1007/978-3-030-94155-0_10

Kumar, V., Baweja, M., Singh, P., Rawat, P. and Rathi, B., 2020. Nano-encapsulation in plant disease management. Crit. Rev. Biotechnol., 40(5): 682–699.

Kumar, V., Naik, I.S., Das, B., Singh, A., Nayak, P., Mohapatra, C., Debnath, D., Tripathy, M., Behera, K., Masika, F.B. and Manohar, S., 2025. Nanoparticles in plant systems. Plant Stress.

Liu, Y., Liu, K., Wang, X., Shao, Y., Li, X., Hao, L. and Lu, J., 2023. Co-assembling nanoparticles. Food Chem., 402: 134409. https://doi.org/10.1016/j.foodchem.2022.134409

Mahdy, E.E., El-Shimy, A.A., Sayed, M.A., Mahmoud, A.F. and Salah, A., 2023. Sesame tolerance to *Macrophomina phaseolina*. Egypt. J. Agron., 45(1): 31–44.

Maxwell, M., and Bateman, B. 1967. Changes in the activities of some oxidases in extracts of Rhizoctonia-infected bean hypocotyls in relation to lesion maturation: 132-136.

McCready, R.M., Guggolz, J., Silviera, V. and Owens, H.S., 1950. Determination of starch and amylose. Anal. Chem., 22(9): 1156–1158. https://doi.org/10.1021/ac60045a016

Mendes, B.B., Conniot, J., Avital, A., Yao, D., Jiang, X., Zhou, X., Sharf-Pauker, N., Xiao, Y., Adir, O., Liang, H. and Shi, J., 2022. Nanodelivery of nucleic acids. Nat. Rev. Methods Primers, 2(1): 24. https://doi.org/10.1038/s43586-022-00104-y

Nedved, E.L., Kalatskaja, J.N., Ovchinnikov, I.A., Rybinskaya, E.I., Kraskouski, A.N., Nikalaichuk, V.V. and Laman, N.A., 2022. Chitosan under salt stress. Appl. Biochem. Microbiol., 58(1): 69–76. https://doi.org/10.1134/S0003683822010069

Nguyen, T.H.A., Doan, V.D., Tran, A.V., Nguyen, V.C., Nguyen, A.T. and Vasseghian, Y., 2022. ZnO nanocomposite synthesis. Mater. Lett., 308: 131129. https://doi.org/10.1016/j.matlet.2021.131129

Nurah, M., Taha, E.M., Bakr, A.A. and Loutfy, N., 2022. Oilseed production in Egypt. J. Oilseed Res., 39(4): 456–470.

Rahman, A.N.A., Shakweer, M.S., Algharib, S.A., Abdelaty, A.I., Kamel, S., Ismail, T.A., Daoush, W.M., Ismail, S.H. and Mahboub, H.H., 2022. Silica nanoparticle toxicity. Aquac. Rep., 23: 101034. https://doi.org/10.1016/j.aqrep.2022.101034

Rai, M. and Ingle, A., 2012. Role of nanotechnology in agriculture with special reference to management of insect pests. Appl. Microbiol. Biotechnol., 94(2): 287–293. https://doi.org/10.1007/s00253-012-3969-4

Rajeevan, R., Maity, S., Nayak, Y., Narayan, R.,

Mehta, C.H., Kamath, P.P. and Nayak, U.Y., 2023. Development of nanostructured lipid carriers loaded caffeic acid topical cream for prevention of inflammation in wistar rat model. J. Appl. Pharma. Sci., 13(1): 064-075.

Ramzan, M., Haider, S.T.A., Hussain, M.B., Ehsan, A., Datta, R., Alahmadi, T.A. and Alharbi, S.A. 2024. Kaempferol and caffeic acid under salinity stress. Sci. Rep., 14(1): 21657. https://doi.org/10.1038/s41598-024-72420-0

Raza ZA, Khalil S, Ayub A, Banat IM., 2020. Recent developments in chitosan encapsulation of various active ingredients for multifunctional applications. Carbohydr. Res., 492: 108004. https://doi.org/10.1016/j.carres.2020.108004

Riaz, U., Kharal, M.A., Murtaza, G., Zaman, Q., Javaid, S., Malik, H.A. and Abbas, Z., 2019. Prospective roles and mechanisms of caffeic acid in counter plant stress: A mini review. Pak. J. Agric. Res., 32(1): 8. https://doi.org/10.17582/journal.pjar/2019/32.1.8.19

Samy, A.M., Mahmoud, A.F. and Abdalla, O.A., 2025. Trichoderma control of charcoal rot. Sultan Qaboos Univ. J. Sci., 30(1): 35–43. https://doi.org/10.53539/2414-536X.1400

Shoala, T., El-Garhy, H.A., Messiha, N.A. and El-Abeid, S.E., 2025. Nanoparticles and soil biodiversity. BMC Microbiol., 25(1): 305. https://doi.org/10.1186/s12866-025-04022-3

Shoukat, A., Pitann, B., Zafar, M.M., Farooq, M.A., Haroon, M., Nawaz, A. and Saqib, Z.A., 2024. Nanotechnology for climate change mitigation: Enhancing plant resilience under stress environments. J. Soil Sci. Plant Nutr., 187(5): 604-620. https://doi.org/10.1002/jpln.202300295

Thimmaiah, S.K., 1999. Standard methods of biochemical analysis. New Delhi: Kalyani Publishers.

Wang, F., Li, L., Iqbal, J., Yang, Z. and Du, Y., 2022. Magnetic chitosan biochar adsorption. Int. J. Biol. Macromol., 199: 234–242. https://doi.org/10.1016/j.ijbiomac.2021.12.195

Wang, J.Z., Yan, C.H., Zhang, X.R., Tu, Q.B., Xu, Y., Sheng, S., Wu, F.A. and Wang, J., 2020. A novel nanoparticle loaded with methyl caffeate and caffeic acid phenethyl ester against *Ralstonia solanacearum* (a plant pathogenic bacterium). RSC Adv., 10: 3978–3990. https://doi.org/10.1039/C9RA09441E

Yalouskaya, N.A., Kalatskaja, J.N., Laman, N.A., Nikalaichuk, V.V., Kraskouski, A.N. and Hileuskaya, K.S., 2023. Caffeic acid in potato microclones. Appl. Biochem. Microbiol., 59(5): 686–693. https://doi.org/10.1134/S0003683823050046

Yousef, H., 2021. Bioagents for powdery mildew control. Egypt. J. Agric. Res., 99(2): 158–169. https://doi.org/10.21608/ejar.2021.70835.1099

Youssef, F.S., Mohamed, G.G., Ismail, S.H., Elzorba, H.Y., Galal, A.M. and Elbanna, H.A., 2021. Florfenicol-chitosan nanocomposite. Egypt. J. Chem., 64(2): 941–948.

Zahin, M., Ahmad, I. and Aqil, F., 2017. Antioxidant potential of *Psidium guajava*. Drug Chem. Toxicol., 40(2): 146–153. https://doi.org/10.1080/01480545.2016.1188397

Zieslin, N. and Ben-Zaken, R., 1993. Peroxidase activity in rose flowers. J. Plant Physiol., 142: 309–315.

Zhou, J., Tu, M., Mao, M., Hu, Q., Dong, Y., Luo, Z. and Li, L., 2024. Tryptophan as a potential way to enhance phenolics accumulation in strawberry: From perspective of phenolomics. Food Biosci., 62: 105370.